Optical Coherence Tomography (OCT) is an interferometric optical imaging technique capable of imaging tissue microstructure at near histological resolutions [1]. Unfortunately, the linear scattering properties of pathological tissue probed by OCT are often morphologically and/or optically similar to normal tissue. To address this problem novel contrast methods for OCT have been recently developed, such as spectroscopic OCT [2], a pump and probe technique [3], and the use of engineered microspheres [4] or microbubbles [5].

Spectroscopic OCT (SOCT) measures the spectral absorption from tissues by measuring the spectral differences between the source and the backscattered interference signal to provide information about the properties of the scatterers in the sample. However, this technique is limited to the identification of scatterers that have absorption within the bandwidth of the optical source. A different method to obtain contrast enhanced OCT employs engineered microsphere contrast agents, which can be targeted to cell receptors thereby providing molecular specific contrast [4]. A drawback to this technique, however, is that the contrast agents may negatively impact the biology under investigation. We present a new method for achieving enhanced OCT contrast, exploiting the inherent vibrational frequency differences between molecular bonds within the tissues. The spectroscopic technique that is employed to detect these vibrational differences is Coherent Anti-Stokes Raman Scattering (CARS).

CARS is a well-known spectroscopic technique that has recently received significant attention for its applications to scanning microscopy. In CARS spectroscopy, the frequencies of two incident lasers, ω_p (pump) and ω_s (Stokes), are chosen such that the difference $\omega_p - \omega_s = \omega_v$ is equal to a Raman-active vibrational mode of the molecule under study [6]. CARS is a non-linear, four-wave mixing process. Furthermore, the CARS field is a result of the interaction between four photons and is generated in the phase-matching direction at the anti-Stokes frequency $\omega_{AS} = 2\omega_p - \omega_s$, implying that the CARS signal intensity is linearly dependent on the Stokes field intensity and quadratically dependent on the pump field intensity. Note that, in addition to the CARS signal, a broadband non-resonant background is always present, limiting the vibrational contrast achieved in CARS microscopy. However, CARS is a coherent process, with the phase of the anti-Stokes field deterministically related to the phase of the excitation field. Therefore, constructive interference of the anti-Stokes field causes the CARS signal to be significantly larger than the spontaneous Raman signal, given the same average excitation power [7]. All these characteristics have allowed CARS to be successfully employed to provide vibrational contrast in scanning microscopy [7, 8, 9, 10, 11].

CARS scanning microscopy generally involves scanning overlapped and tightly focused pump and Stokes lasers through a sample while measuring the anti-Stokes signal amplitude point by point. The first CARS microscope [8] utilized non-collinear pump and Stokes visible lasers to demonstrate microscopic imaging of the spatial distribution of deuterated molecular bonds in a sample of onion skin. Tightly focused, collinear near-infrared pump and Stokes pulses were used [9] to achieve improved background signal suppression, and three-dimensional sectioning in living cells. In each of these CARS microscopy techniques, the anti-Stokes photons are counted in order to estimate the density of the Raman scatterers and/or Raman susceptibility magnitude in the focal volume of

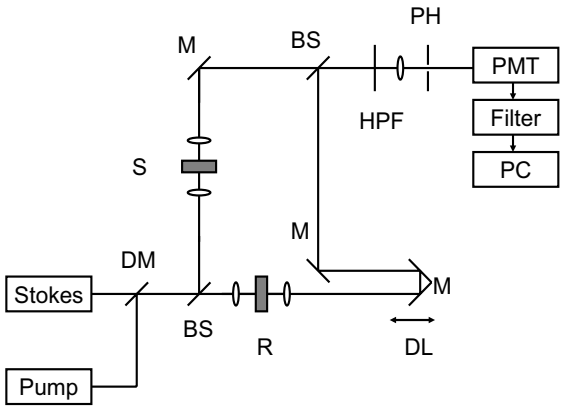

FIG. 1: Schematic of the interferometric CARS measurement system. Benzene was used for both the reference and sample materials in this study. Abbreviations: S, sample; R, reference; DM, dichroic mirror; BS, beamsplitter; M, mirror; HPF, high-pass-filter; PH, pin-hole; DL, delay line.

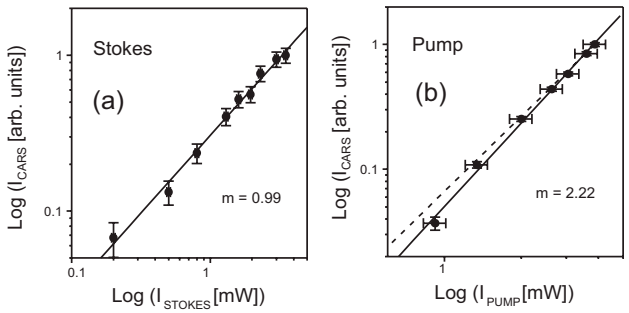

FIG. 2: Intensity of the CARS signal as a function of (a) the intensity of the Stokes field and (b) the intensity of the pump field. Both figures are log-log plots and the solid lines represent curve fitting. The dotted line of Fig.2(b) has a slope of 2. The parameter m is equal to the angular coefficient of the solid lines.

the microscope. However, the spectral phase information is lost in this process and can only be inferred. In this Letter we propose and demonstrate a new CARS interferometric technique called Nonlinear Interferometric Vibrational Imaging (NIVI) with the capability for heterodyne detection and the possibility to obtain a full reconstruction of the magnitude and phase of the sample Raman susceptibility.

The CARS interferometer described in this paper is presented in Fig.1. An excitation field consisting of two overlapped pulses centered at the pump and Stokes wavelengths is divided by a beamsplitter into two separate interferometer paths, which are referred to in Fig.1 as arm "S" (or sample arm) and arm "R" (or reference arm). A sample of a molecule is placed into each arm into which the split excitation fields are focused. If the frequency difference between the pump and Stokes pulses is tuned to a Raman active vibrational mode present in both sample S and sample R, an anti-Stokes signal is generated in each arm of the interferometer. Because the anti-Stokes pulse phase is deterministically related to the phase of the pump and the Stokes pulses, the anti-Stokes fields are coherent with the excitation fields and also with each other. It follows (Feynman principle) that when these anti-Stokes fields are temporally and spatially overlapped, interference can be observed.

In our current setup the CARS is stimulated by a laser system similar to that employed by [9]. A diode pumped frequency doubled Nd:YVO_4 laser is used to pump a mode-locked Ti:sapphire oscillator operating at a center wavelength of 807 nm, with a bandwidth of 30 nm, a repetition rate of 82 MHz, and an average power of 300 mW.

These pulses seed a regenerative chirped pulse amplifier (Coherent, RegA 9000) producing approximately 70 fs, 5 J pulses at a repetition rate of 250 kHz with an average power of 1.25 W. Ten percent of this average power is used as the pump beam while the remaining power is directed to an optical parametric amplifier (Coherent, OPA 9400) which generates a 4 mW average power Stokes beam, tunable from 400-1200 nm.

The pump and Stokes pulses, at 807 and 1072 nm respectively, are used to excite the strong, isolated Raman-active vibrational mode of benzene at 3063 cm^{-1}. As shown in Fig.1, these pulses are collinearly overlapped using a dichroic mirror and split with a 50:50 ultrafast beamsplitter into arms S and R. In each arm, a 30 mm focal length, 12 mm diameter achromatic lens is used to focus the pump and Stokes beams into a quartz cuvette filled with benzene. The anti-Stokes signals generated in each arm are collected in the collinear phase matching direction using 30 mm focal length, 12 mm diameter singlet lenses. The two anti-Stokes pulses are overlapped in time by adjusting the relative delay and in space by adjusting the position on a second beamsplitter. A high-pass filter at 742 nm eliminates the remaining excitation light. The filtered anti-Stokes signal is spatially filtered through a 50 m diameter pin hole. The relative delay is scanned by a computer-controlled single axis translation stage at a constant rate in arm R, and the CARS signal intensity is measured with a photomultiplier tube PMT (Hamamatsu, HC 123). Lastly, the signal from the PMT is filtered with a low-pass anti-aliasing filter and sampled with a PC based data acquisition system.

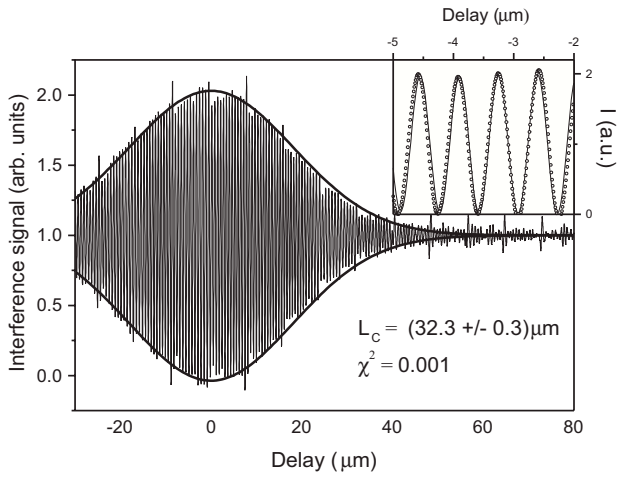

FIG. 3: CARS interferogram detected at the beamsplitter BS and produced as the pathlength of arm R is scanned. The modulus of the degree of the coherence function is used to fit to the envelope of the interferogram. The inset shows an enlarged version of the interference pattern and its fit by the real part of the degree of coherence function. L_C is the coherence length of the CARS pulse.

Figures 2(a) and 2(b) show the observed relationship between the CARS and the Stokes intensity (pump intensity fixed) and the CARS and the pump intensity (Stokes intensity fixed), respectively. The solid lines represent linear fits of the experimental data. In agreement with theory, the slope of the fitted lines verifies the linear relationship between the anti-Stokes and the Stokes intensities and the quadratic relationship between the anti-Stokes and the pump intensities. Our signal is therefore a result of a four-wave mixing process. Moreover, this process is CARS resonance because the anti-Stokes power is maximized when the Stokes wavelength is tuned to resonance with the Raman-active benzene vibrational mode.

Fig.3 contains the measured interferogram resulting from the interference between the two anti-Stokes signals at the beamsplitter BS. The real part and the modulus of the coherence function, for the case of a Gaussian spectral distribution, are used to fit the experimental data (interferogram and envelope respectively). The resulting coherence length L_C, or the axial resolution of the interferometric CARS measurement technique, is found to be equal to (32.3 +/- 0.3) μm (reduced $\chi^2 = 0.001$).

The inset of Fig.3 shows an enlarged version of the interferogram fringes. Open circles correspond to the experimentally measured data and the solid line represents a fit of the data. This result indicates that two anti-Stokes signals generated in separate samples can be demodulated interferometrically, where the amplitude of the fringe envelope gives information about the concentration of the scatterers in the focal volume of the sample objective lens. The presence of interference clearly demonstrates the potential of CARS as a promising technique for providing molecular contrast for OCT-like interferometric imaging systems. In fact, the presence of the interference indicates that similar Raman-active vibrational frequencies are present in both the reference and the sample arm at the same path length from the detector. The "fingerprint" nature of Raman spectroscopy, combined with the possibility to switch between different samples in arm R, could permit selective detection and imaging, within the above mentioned axial resolution, of different molecular species present in the sample S.

Note finally that the interferometric detection scheme could provide numerous advantages over traditional photon counting CARS microscopy. Interfering a weak CARS signal with another strong CARS signal, can provide heterodyne sensitivity for improved S/N ratio. Moreover, with full knowledge of the excitation pulses and of the CARS interferogram, the spectral amplitude and the phase of the CARS pulse can be measured. A complete reconstruction of the Raman susceptibility may then be attained allowing for a more accurate molecular identification [12].

In conclusion, we have described a new technique for CARS measurement that relies on the deterministic nature of the CARS process. The interference between two CARS signals, generated in separate samples, was observed allowing for heterodyne detection. This result is extremely promising for the development of a new molecular imaging technique (NIVI) based on non-linear, low-coherence interferometry. While this demonstration used forward CARS, epi-detected CARS [7] is coherent as well, and is compatible with OCT coherence-ranging systems. CARS interferometry provides CARS microscopy the advantages of interferometric detection and provides OCT with molecular-specific contrast. These advantages could make CARS interferometry a powerful tool for biological imaging with OCT and for disease diagnosis at the molecular level.

This research was supported in part by a research grant entitled "A Nonlinear OCT System for Biomolecular Detection and Intervention" from NASA and the National Cancer Institute (NAS2-02057, SAB). S.A. Boppart's email address is boppart@uiuc.edu.

* Electronic address: boppart@uiuc.edu

[1] S. A. Boppart, B. E. Bouma, C. Pitris, J. F. Southern, M. E. Brezinski, and J. G. Fujimoto, "In vivo cellular optical coherence tomography imaging," *Nature Medicine.*, vol. 4, no. 7, pp. 861–5, 1998.

[2] U. Morgner, W. Drexler, F. Kartner, X. Li, C. Pitris, E. Ippen, and J. Fujimoto, "Spectroscopic optical coherence tomography," *Optics Letters*, vol. 25, no. 2, pp. 111–

13, 2000.

[3] K. Divakar Rao, M. A. Choma, S. Yazdanfar, A. M. Rollins, and J. A. Izatt, "Molecular contrast in optical coherence tomography by use of a pump-probe technique," *Optics Letters*, vol. 28, no. 5, pp. 340–2, 2003.

[4] T. M. Lee, A. L. Oldenburg, S. Sitafalwalla, D. L. Marks, W. Luo, F. J.-J. Toublan, K. S. Suslick, and S. A. Boppart, "Engineered microsphere contrast agents for optical coherence tomography," *Optics Letters*, vol. 28, no. 17, pp. 1546–1548, 2003.

[5] J. K. Barton, J. B. Hoying, and C. J. Sullivan, "Use of microbubbles as an optical coherence tomography contrast agent," *Academic Radiology.*, vol. 9, no. Suppl 1, pp. S52–5, 2002.

[6] W. Dermtroeder, *Laser Spectroscopy.* Springer, 1998.

[7] J.-X. Cheng, A. Volkmer, and X. Xie, "Theoretical and experimental characterization of coherent anti-stokes raman scattering microscopy," *Journal of the Optical Society of America B (Optical Physics)*, vol. 19, no. 6, pp. 1363–75, 2002.

[8] M. Duncan, J. Reintjes, and T. Manuccia, "Scanning coherent anti-stokes raman microscope," *Optics Letters*, vol. 7, no. 8, pp. 350–2, 1982.

[9] A. Zumbusch, G. Holtorn, and X. Sunney Xie, "Three-dimensional vibrational imaging by coherent anti-stokes raman scattering," *Physical Review Letters*, vol. 82, no. 20, pp. 4142–5, 1999.

[10] G. W. Wurpel, J. M. Schins, and M. Muller, "Chemical specificity in three-dimensional imaging with multiplex coherent anti-stokes raman scattering microscopy," *Optics Letters*, vol. 27, no. 13, pp. 1093–1095, 2002.

[11] M. Hashimoto, T. Araki, and S. Kawata, "Molecular vibration imaging in the fingerprint region by use of coherent anti-stokes raman scattering microscopy with a collinear configuration," *Optics Letters*, vol. 25, no. 24, pp. 1768–1770, 2000.

[12] D. L. Marks and S. A. Boppart, "Nonlinear interferometric vibrational imaging," *Submitted*, E-print@arxiv.org/physics/0311071, http://www.arxiv.org/abs/physics/0311071, 2003.